

Nanosecond Gated Raman Spectroscopy for Standoff Detection of Hazardous Materials

Jin Hyuk Chung and Soo Gyeong Cho*

Institute of Defense Advanced Technology Research, Agency for Defense Development (ADD), Daejeon 305-600, Korea

**E-mail: soochol1@nate.com*

Received July 30, 2014, Accepted August 18, 2014

Laser Raman spectroscopy is one of the most powerful technologies for standoff detection of hazardous materials including explosives. Supported by recent development of laser and sensitive ICCD camera, the technology can identify trace amount of unknown substances in a distance. Using this concept, we built a standoff detection system, in which nanosecond pulse laser and nanosecond gating ICCD technique were delicately devised to avoid the large background noise which suppressed weak Raman signals from the target sample. In standoff detection of explosives which have large kill radius, one of the most important technical issues is the detection distance from the target. Hence, we focused to increase the detection distance up to 54 m by careful optimization of optics and laser settings. The Raman spectra of hazardous materials observed at the distance of 54 m were fully identifiable. We succeeded to detect and identify eleven hazardous materials of liquid or solid particles, which were either explosives or chemical substances used frequently in chemical plants. We also performed experiments to establish the limit of detection (LOD) of HMX at 10 m, which was estimated to be 6 mg.

Key Words : Raman spectroscopy, Standoff detection, Nanosecond gating, Hazardous material, Explosives

Introduction

Standoff detection of hazardous materials is of significant importance in the area of security and surveillance. Particularly, recent examples in Iraq and Afghanistan wars showed that detection of explosives including improvised explosive devices (IEDs) in a relatively safe distance was important to protect armed personnel. It was reported that almost half of the casualties of American soldiers in Iraq and Afghanistan wars were caused by IEDs.¹ Considering kill radius of explosives, securing safe distance on detection is essential. Safe distance varies depending upon the amount of explosive materials to be detected. In case of IEDs carried by a terrorist, the safe distance is considered to be 10 m. However, the safe distance for IED loaded in a vehicle is substantially longer than this. Consequently, it is much better to have a long detection distance in standoff system. Besides military application, Raman standoff technique may also be useful to detect leaking hazardous materials from chemical plants, and to protect workers in the plant and nearby residents.

The advantage of Raman is fast recognition and trace tracking which requires only small amount of target material. In addition to it, regarding the potential deployment in a civilian area, Raman technology requires comparatively low laser energy to induce the scattering, while X-ray technology in standoff detection requires much higher energy. In X-ray, the control of intensity should be carefully elaborated not to harmfully affect the health of human being scanned. Together with the virtues of laser including straight propagation and agile delivery of optical information in light speed, laser

Raman scattering could make a useful tool for standoff detection.

In the meanwhile, a known disadvantage of Raman is inherently weak intensity which makes the Raman signals easily overwhelmed by background noises. For example, even a small indoor light has much higher intensity than Raman scattering. In an observation under such a condition, Raman signals could disappear in the background noise easily. However, since nanosecond pulse laser can generate numerous photons in a pulse whose time width is less than 10 ns, and ICCD camera of modern technology can control the duration of shutter opening time in the order of few nanoseconds, the nanosecond gated laser Raman system can be built up for blocking the background noises coming from the environment. With such a system, shooting a chunk of photons in a nanosecond time scale can induce Raman scattering in such a time, then the ICCD camera can be controlled to accept the signal only within a similar time scale.

Experimental Section

The detailed specification of the standoff Raman system was described elsewhere.² The standoff system was composed of five parts including reflective telescope, Nd:YAG laser, spectrometer, ICCD camera, and analyzing computer. Since Raman signal was scattered to all directions isotropically and larger scattering cross section coverage was preferred, a reflective telescope with wider diameter was adopted for design concept. The reflective scope of 310 mm diameter with a modified optical adapter at the position of

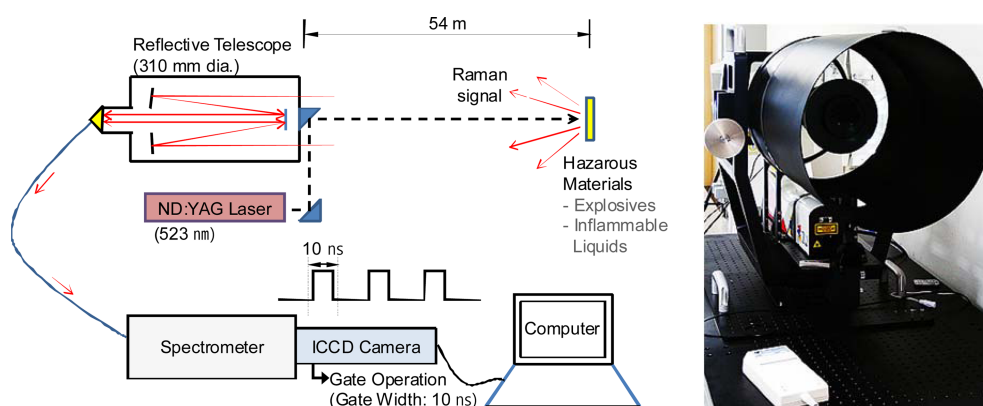


Figure 1. The standoff Raman detection system with 310 mm diameter reflective telescope and 10 ns Nd:YAG laser.

the eyepiece was built manually for the specific standoff Raman detection purpose. There were some standoff Raman systems previously reported in other researches.³⁻⁵ Not like most of these systems which adopted modification of retail telescope originally devised for visible observation, our system was optimally designed solely for Raman scattering detection. The positioning of lenses was chosen for effective concentration of Raman photons regarding laser beam width and expected scattering cross section. The size of final focus point was also adjusted for photon collecting method using optical fiber. The standoff Raman system is shown in Figure 1.

The 532 nm, 10 Hz, Nd:YAG laser with maximum pulse energy of 160 mJ/pulse was installed below the reflective telescope and the optical path of the laser beam was aligned to be identical to the optical path of the telescope for the optimal reception of Raman signals. The beam spot of the laser was adjusted to be located at the center of the field of view of the telescope. In the spectrometer, PI Acton 2500i, Raman signals were turned into spectrum in the range of 800–3600 cm^{-1} . This spectrum information was read by ICCD camera PI-MAX3 with resolution of 1024×256 . The ICCD camera was synchronized with the laser to open the shutter and receive the signals at some specific time after the pulse laser was triggered. For the purpose of blocking background noise, the shutter was always controlled to be open for 10 ns only when Raman signals reached the camera. For different standoff distance, this time delay was re-calculated to be input into the system. The measured data were displayed on the computer.

Measurements

Raman signals of eleven hazardous materials were measured by standoff Raman system. Target materials included five solid explosive molecules in a form of powder, namely TNT, RDX, HMX, PETN, and TATP (See the Fig. 2), one liquid explosive, nitromethane, one liquid explosive stimulant, nitrobenzene, and four inflammable liquids, *i.e.* acetone, acetonitrile, ethanol, methanol. The explosive molecules chosen for this work covered most of explosive molecular types used in IEDs. TNT represents nitroaromatics, whereas RDX and HMX belong to nitramines. PETN and TATP are

nitroester and peroxide, respectively. Nitromethane is liquid, as mentioned previously. All the samples were put in a quartz cell which was known to have no major Raman scattering in the range of interest for the experiment.⁶ The size of quartz cell was $10 \times 10 \times 45$ mm. The quartz cells were put on a platform located standoff distance away from the telescope system. After the incident green laser pulse with 532 nm wavelength hit the target sample at standoff distance, the back scattered Raman signals were collected by telescope and got passed to spectrometer by optical fiber attached to the focal plane of the system. Pulse energy of laser which was measured at the standoff distance was fixed to be 30 mJ/pulse preventing possible detonation. For each measurement, minimum 300 pulses were irradiated on a target sample and Raman signals were accumulated to produce more accurate data and to reduce random noise background. For each laser pulse with 5 ns width, the shutter of ICCD camera was opened for 10 ns only to accept the signal. Balancing the higher sensitivity of data and growing noise, the gain of ICCD was kept on 70 in the measurements at 30 m. For indoor measurement, the experiments were performed in both conditions of fluorescent lights on and off. In case of both of 30 and 54 m measurements, target samples and standoff system were moved to outdoor under the sun for inspecting the contribution of the sunray. Unless specified, all of the acquired standoff data were pretreated with simple statistical method to remove constant background noise. For confirming the standoff Raman signal of

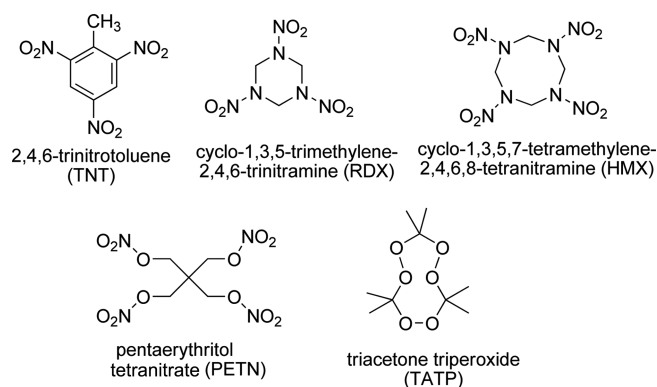


Figure 2. Solid explosive molecules studied in this work.

the target material, the Raman spectra of all the materials studied in this work were measured with confocal Raman microscope, Alpha300R of WiTeK, and Kaiser optics MR. Probe, with 532 nm continuous laser in close distance.

Due to the nature of isotropic scattering, the observed Raman signals in the measurements of 54 m distance became much weaker. For example the amount of Raman signals at 54 m was calculated to be about 3.4% of that at 10 m. To compensate this loss and acquire better signals, additional optimization methods were applied to the standoff system. In 54 m data taking, the gain of ICCD gate opening was increased to 80 for higher sensitivity. Gate exposure, the number of data accumulation for one measurement, was typically 300 in 30 m. However, in 54 m measurement, data had to be taken up to 1,000 times in some cases where the intensity was so low. Additionally, the gate delay, the time duration from laser trigger to ICCD gate opening, had to be best optimally chosen for maximum signal. Depending on the opening timing of ICCD, the acquired amount of Raman signal was changed significantly. In case of 54 m measurement, all the values in the range from 337 to 375 ns in each step of 0.5 ns increments were tested for the highest signal, which loaded to 365 ns for the final measurement.

Another essential improvement was performed by accurate alignment of optical path. In the reflective telescope, the Raman photons converged on an optical fiber at the focal plane. Since the diameter of fiber core was 100 μm , focusing the Raman signals on the focal plane and positioning the fiber at the focal point had to be precise. To achieve this accuracy, fiber optics were modified to control the standoff system. Instead of manual linear movement of fiber part, rotational control method was installed to find the focal plane. Using this method, optical fiber position could be controlled in the precision of 2 μm , which improved the signal intensity significantly.

Results and Discussion

The measured confocal Raman signals of TNT, RDX, HMX, PETN, and TATP were compared with previously reported results.⁷⁻¹² All of them provided near identical results in major peaks although there were small discrepancies due to the calibration and systematic errors. The standoff Raman results of these explosives at 30-54 m distance were compared with confocal result as shown in Figure 3. For each plot in the figure, the spectrum in the bottom represented the confocal result, while those in the middle and top depicted 30 m and 54 m results. All the plots were in arbitrary unit to compare peak locations easily. To reduce background noises, all the data were processed with Savitzky-Golay filter.¹³ It minimized the random noise peaks which were inevitably picked up by the optical system. In addition, a rolling ball method was applied to reduce baseline noises induced from the optical apparatus and inherent fluorescence of target molecules.

Some materials had strong fluorescence, which hindered from detecting weak Raman signals. For example, RDX and

TNT had strong fluorescence which could be confirmed in the standoff data. Due to this effect, even if most of the fluorescence could be removed after the background pretreatment process, many weak Raman peaks were also eliminated and numerous small noise peaks were still observable as shown in Figure 3(a) and 3(b). Compared to standoff data, confocal data had advantage of removing most of fluorescence due to the inherent confocal function in 2D scan.

Compared to confocal data which had advantages of fluorescence removal and low noise configuration, Raman results at both 30 m and 54 m had lower signal intensity and larger noise peaks in the baseline. This condition made some peaks located quite close to the other merge into one. It also caused slight shift of peaks or missing peaks occasionally. However, most of the data showed good enough peak characteristics of each material for identification. For example, in case of standoff TNT measurements plotted in Figure 3(a), in spite of slight peak shifting and large fluorescence eliminating small peaks, the representative peaks were successfully observed at 1365 cm^{-1} (strongest), 1215 cm^{-1} , 1527 cm^{-1} , and 1612 cm^{-1} . The largest one at 1361 cm^{-1} was reported to be induced from symmetric stretching mode of the C-N bond connected to 4- NO_2 group. RDX had two peak groups which were around 1230 cm^{-1} and 3000 cm^{-1} . In 54 m standoff observation shown in Figure 3(b), RDX which had many noise peaks due to the fluorescence showed a wide peak at 1241 cm^{-1} , which seemed to be a merged one of few original peaks around 1230 cm^{-1} . However, another RDX specific group of 3 peaks at 2958 cm^{-1} , 3004 cm^{-1} , and 3071 cm^{-1} was clearly able to be identified. Observing the peak group in the range from 2900 cm^{-1} to 3100 cm^{-1} , it could be noticed that our sample was α polymorph. In the 54 m data (top in Fig. 3(c)), HMX also had a merged peak at 3013 cm^{-1} , which was used to be two peaks at 2996 cm^{-1} , and 3034 cm^{-1} of the 30 m data. There were also some shifts of other peaks, for example, peaks originally at 1247 cm^{-1} , and 1303 cm^{-1} got shifted slightly. However, overall shape of the Raman spectrum was not changed. Being β polymorph, the largest peak was observed at 836 cm^{-1} as expected. Similar phenomena were also observed in the case of PETN as shown in Figure 3(d). Two peaks located close around 3003 cm^{-1} were merged as one, and the rest of the peaks got broadened. The second largest peak at 1318 cm^{-1} was well observed as reported previously by Gaft *et al.*¹¹ TATP was comparatively easy to produce and composed of inexpensive ingredients, which made its growing usage in terrorist activities recently. Two large peaks were shown well around 2912 cm^{-1} in 30 m spectrum, but were merged in 54 m spectrum. Second largest peak around 1155 cm^{-1} , which was shown in 30 m measurement, was disappeared in 54 m measurement as shown in Figure 3(e). The overall spectrum shape of TATP in our standoff measurements was quite similar to the one reported previously by Oxley *et al.*¹² We believed that the overall spectrum shapes of these explosive molecules remained robust enough to identify each explosive, in spite of some losses and defects.

In case of liquid samples, as shown in Figure 4, not like

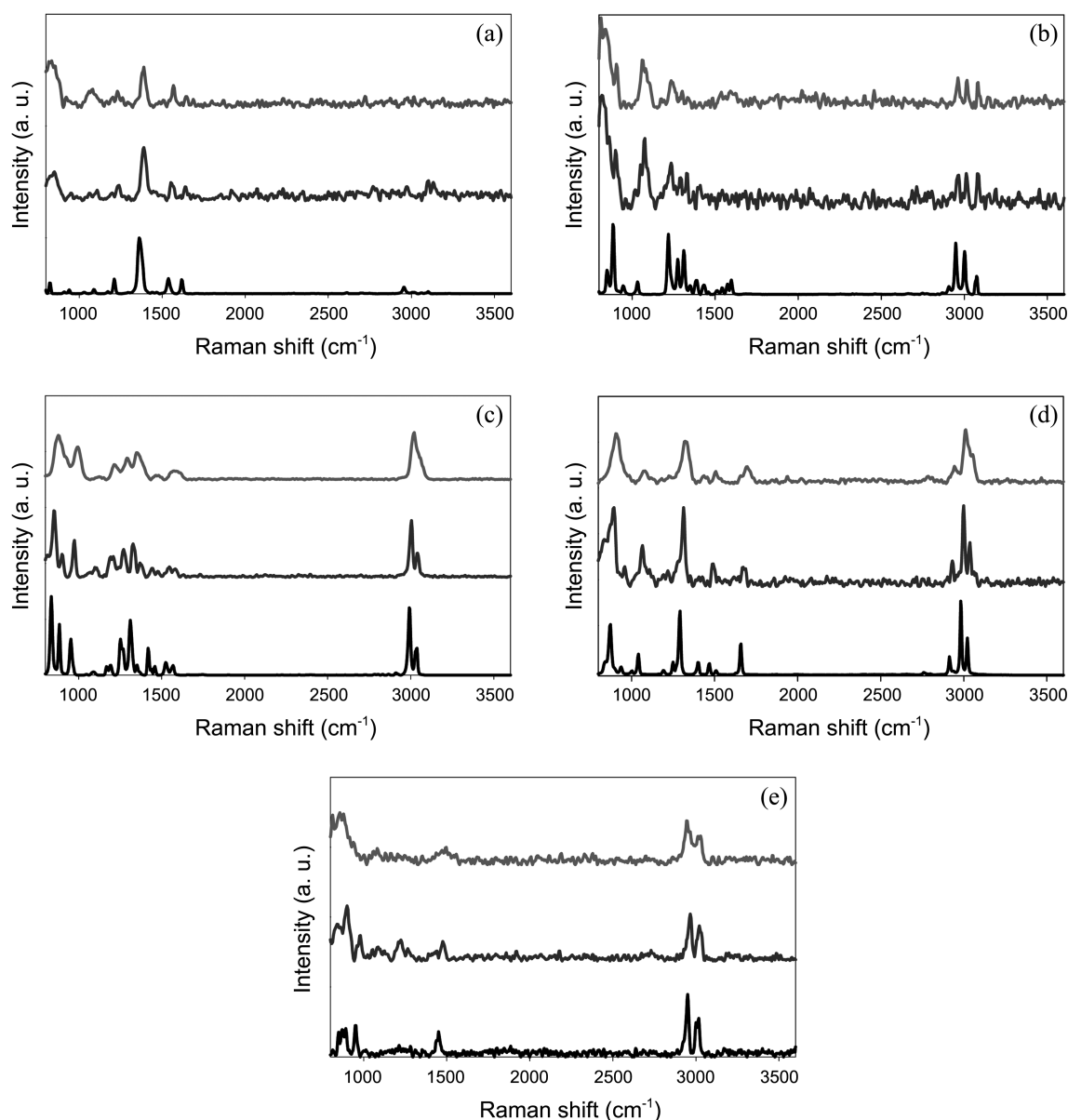


Figure 3. Raman spectra of (a) TNT, (b) RDX, (c) HMX, (d) PETN, and (e) TATP measured by confocal microscope (bottom), and by a standoff system at 30 m (middle) and at 54 m (top).

solid materials, each Raman spectrum had only a few peaks located close to each other. Hence, there were not many peaks which got possibly merged in 54 m data. Such a condition would be an advantage for better identification of liquid samples. However, the absolute amounts of Raman intensities of liquid samples were smaller than those of solid samples in general, which caused misreading of peaks sometimes. Acetone, a strong inflammable liquid and used in chemical plants frequently, had strongest peak at 2928 cm^{-1} , which could be observed in Figure 4(a) in all the observations. Both of 30 and 54 m data of acetonitrile in Figure 4(b) showed the characteristic peaks at 2248 cm^{-1} , and 2937 cm^{-1} . Ethanol had three peaks located close at 2890 cm^{-1} , 2937 cm^{-1} , and 2979 cm^{-1} in 30 m data. They were merged into a big peak around 2900 cm^{-1} at 54 m detection (Fig. 4(c)). Second strong peak around 1426 cm^{-1} was also able to be

observed with low sharpness at 54 m data. Methanol was known to have characteristic peaks at 2826 cm^{-1} and 2936 cm^{-1} . Both of peaks were observed in standoff measurements but their intensities decreased in 54 m data (Fig. 4(d)). In Figure 4(e), the notable peaks of nitromethane were at 908 cm^{-1} , 1386 cm^{-1} , and 2975 cm^{-1} , which, in spite of slight shift, were also observed in 54 m data. In Figure 4(f), The strongest peak of nitrobenzene was conspicuous at 1334 cm^{-1} . The peak intensity was much higher than the one reported previously by Pettersson *et al.*⁴ All the secondary peaks around it were clearly detectable, albeit weaker than 30 m, in case of 54 m data.

In order to estimate background noise contribution from ambient light, indoor measurements were performed in conditions with lights on and off. For each of 30 m and 54 m experiments, standoff detection was executed in both indoor

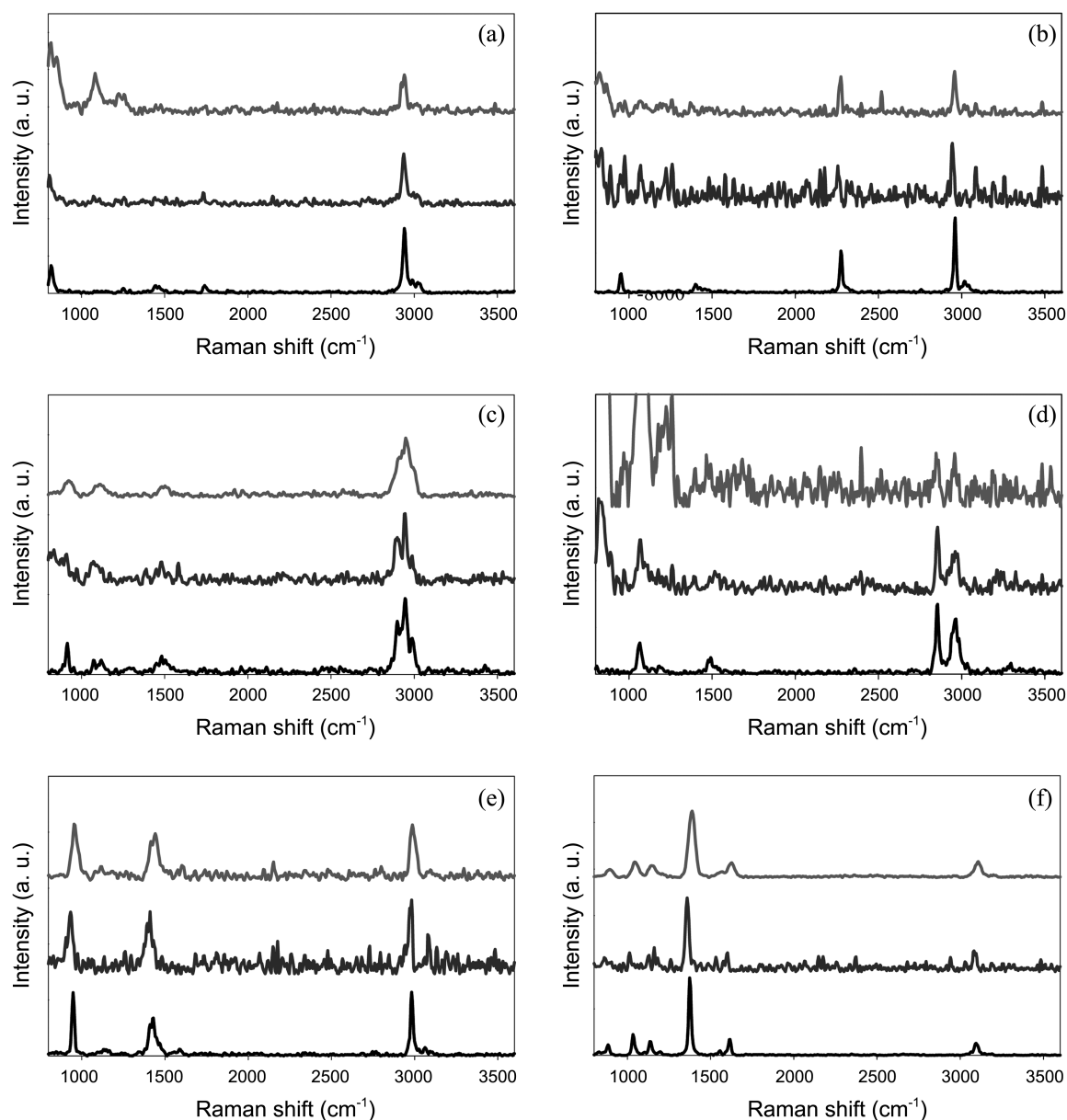


Figure 4. Raman spectra of (a) acetone, (b) acetonitrile, (c) ethanol, (d) methanol, (e) nitromethane, and (f) nitrobenzene measured by confocal microscope (bottom), and by a standoff system at 10 m (middle), and at 54 m (top).

and outdoor conditions under sunray. Figure 5 showed the result of 30 m standoff detection of HMX under two different conditions. There was no difference between the results with indoor light on and off. Even under sunray which provided maximum background noise, experimental results were almost identical regarding the random noise difference and slight signal instability which were observed all the time. Consequently, nanosecond gating technique was quite effective to block the background noise from ambient light.

Every laboratory to perform a research for standoff detection puts much effort to increase the detection distance. However, increasing the detection distance is very difficult because the Raman signals scattered from the explosive materials farther away tend to decrease seriously. Carter *et al.* in Lawrence Livermore National Laboratory performed

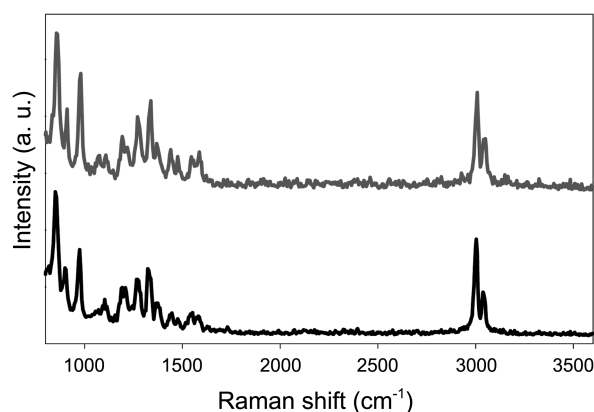


Figure 5. Standoff Raman spectra of HMX at 30 m distance indoor with light off (bottom) and outdoor under sunray (top).

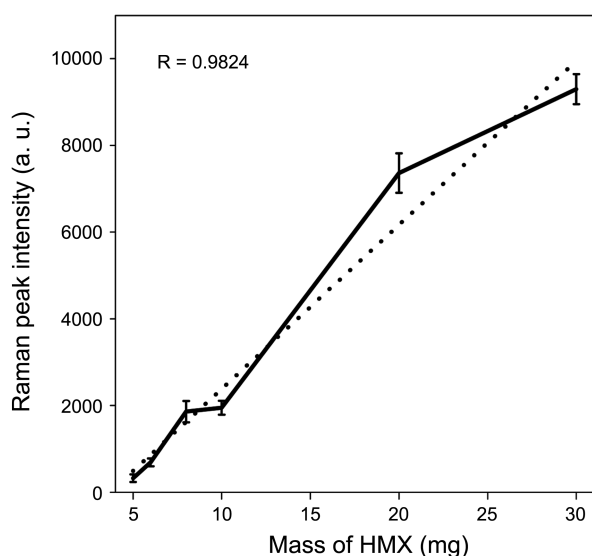


Figure 6. The relationship of the intensity of 3041.5 cm^{-1} at 10 m and the mass of HMX sample (solid line). Corresponding calibration curve is indicated in dashed line. Error bars show the standard deviation from five measurements.

standoff detection of three explosives, namely TNT, RDX, and PETN, using Raman instruments up to 50 m in 2005.¹⁴ They utilized gating control up to 10 ms to remove ambient light influence. In 2009, Pettersson *et al.* in Swedish Defense Research Agency performed standoff Raman study to detect IED precursor materials, which were volatile peroxides and light molecular weight nitro compounds.⁴ In nitrobenzene, the Raman signal (1334 cm^{-1}) measured by Pettersson *et al.* was less than half intensity the one of this work. However, it was quite difficult to evaluate the signal quality because almost all the standoff Raman spectra were generally published in arbitrary scale.

To establish LOD in standoff measurement, the Raman scattering of HMX samples was measured at 10 m distance by changing the amount of HMX in a range from 5 to 30 mg. The sample was put in the quartz cell located on a sample podium. Standoff Raman spectrum was measured five times for each mass under identical configuration of gain, gate delay and gate exposure. The Raman intensity of spectra centered at 3041.5 cm^{-1} was used for the quantitative evaluation of LOD. Figure 6 showed the result which indicated the increasing Raman signal intensity was almost linearly proportional to the mass of the sample. For the evaluation of background noise, the Raman scattering of an empty quartz cell was also acquired in the same condition. Using this information, LOD of HMX at 10 m was evaluated to be 6 mg.

Conclusion

We designed and built a Raman standoff detection system to detect hazardous materials including explosives in a safe distance. With our newly built standoff Raman detection system, Raman signals from various hazardous materials in a safe distance up to 54 m were successfully measured and

analyzed for target identification. To our knowledge, measuring Raman signals above 50 m was achieved by only a few security related laboratories in the world. Going more than 50 m had an importance to show the ability to detect a significantly large amount of hazardous materials including truck fully loaded explosives in a safe distance. In our 54 m experiment, we were able to detect most of the shapes of characteristic peaks were relatively well preserved, and to identify the chemical information well, although there appeared some loss of information including shifted and missing peaks of observed Raman signals. We applied nanosecond gating technique which opened the shutter of ICCD camera only when the Raman signal in nanosecond time width arrived at the detector. With this method, large backgrounds from ambient lights including indoor fluorescent light and outdoor sunray were successfully removed and outdoor standoff detection was able to be performed without background signal contribution. Based on the results of our standoff detection capability, LOD of HMX at 10 m was estimated to be 6 mg. Among tested explosives, a few materials were observed to have large amount of inherent fluorescence hindering Raman signal detection, which should be solved in our future study. Fluorescence not only suppressed some of Raman peaks but also produced substantial background noise. Some methods like lasing with longer wavelength or picosecond gating of ICCD camera were reported to be effective to decrease fluorescence.^{15,16} We are planning to employ these methods in the near future. Applying new methods and optimizing our detection system, we will keep extending the standoff distance for detecting trace amount of hazardous materials including explosives.

References

1. Annual Report FY 2008; Joint Improvised Explosive Device Defeat Organization (JIEDDO), Washington D.C., USA, 2009.
2. Chung, J. H.; Cho, S. G. *Bull. Korean Chem. Soc.* **2013**, *34*, 1668.
3. Efremov, E. V.; Buijs, J. B.; Gooijer, C.; Ariese, F. *Appl. Spectrosc.* **2007**, *61*, 571.
4. Pettersson, A.; Johansson, I.; Wallin, S.; Markus, N.; Ostmark, H. *Propell. Explos. Pyrotech.* **2009**, *34*, 297.
5. Sharma, S. K.; Angel, S. M.; Chosh, M.; Hubble, H. W.; Lucey, P. G. *Appl. Spectrosc.* **2002**, *56*, 699.
6. Gillet, P.; Le Cleach, A.; Madon, M. *J. Geophys. Res.* **1990**, *95*, 21635.
7. Clarkson, J.; Smith, W. E.; Batcheler, D. N.; Smith, D. A.; Coats, A. M. *J. Mol. Struct.* **2003**, *648*, 203.
8. Rice, B. M.; Chabalowski, C. F. *J. Phys. Chem. A* **1997**, *101*, 8720.
9. Brand, H. V.; Rabie, R. L.; Funk, D. J.; Diaz-Acosta, I.; Pulay, P.; Lippert, T. K. *J. Phys. Chem. B* **2002**, *106*, 10594.
10. Goetz, F.; Brill, T. B. *J. Phys. Chem.* **1979**, *83*, 340.
11. Gaft, M.; Nagli, L. *Opt. Mater.* **2008**, *30*, 1739.
12. Oxley, J.; Smith, J.; Brady, J.; Dubnikova, F.; Kosloff, R.; Zeiri, L.; Zeiri, Y. *Appl. Spectro.* **2008**, *62*, 8.
13. Savitsky, A.; Golay, M. J. E. *Anal. Chem.* **1964**, *36*, 1627.
14. Carter, J. C.; Angel, S. M.; Lawrence-Snyder, M.; Scaffidi, J.; Whipple, R. E.; Reynolds, J. G. *Appl. Spectrosc.* **2005**, *59*, 769.
15. Flegler, Y.; Nagli, L.; Gaft, M.; Rosenbluh, M. *J. Lumines.* **2009**, *129*, 979.
16. Akeson, M.; Nordberg, M.; Ehlerding, A.; Nilsson, L.; Ostmark, H.; Strombeck, P. *Proc. SPIE* **2011**, *8017*, 8017C-1.